

DESIGN OF STIFFENED SLABS-ON-GRADE ON SHRINK-SWELL SOILS

J.L. Briaud, R. Abdelmalak and X. Zhang

Zachry Dept of Civil Engineering, Texas A&M University, College Station, Texas 77843-3136, USA;
Geotechnical & Heavy Civil Engineering Department, Dar Al-Handasah., 2 Lebnan St. Mohandessin, Giza,
Cairo, Egypt; Dept. of Civil and Envir. Engineering, University of Alaska, Fairbanks, Alaska 99775, USA

Opening Keynote Lecture, Proceedings of the International Conference on Unsaturated Soils called UNSAT 2010, September 2010 in Barcelona, Spain, CRC Press-Balkema-Taylor and Francis Group.

Abstract:

Stiffened slabs-on-grade are one of the most efficient and inexpensive foundation solutions for light structures on shrink-swell soils. After removing the top soil, the stiffening reinforced concrete beams, say 1m deep and 0.3 m wide, are formed in the natural soil and placed every 3 m in both directions. The slab is typically 0.1 m thick. Such stiffened slabs are often called waffle slabs because of the geometric analogy with a waffle. They are commonly used in the USA for the foundation of houses or any light weight structure on shrink-swell soils and cost about 100\$/m² (2010). This paper presents a simple design procedure and associated charts for calculating the depth of the beams required to limit the differential movement of the foundation due to bending to an acceptable amount. This bending of the foundation is due to the shrinking and swelling of the soil during the dry and wet seasons under the edges of the structure. The procedure consists of using the change in suction or the change in water content selected for design purposes in the region, the anticipate depth of influence of these seasonal changes, the soil properties, and the beam depth, to calculate the distortion of the slab under load. If the distortion is too large for the type of structure considered, the beam depth is increased until the acceptable value is reached.

Introduction

Stiffened slabs-on-grade (Fig.1) are one of the most efficient and inexpensive foundation solutions for light structures on shrink-swell soils. After removing the top soil, the stiffening reinforced concrete beams, say 1m deep and 0.3 m wide, are formed in the natural soil and placed every 3 m in both directions. The slab is typically 0.1 m thick. Such stiffened slabs are often called waffle slabs because of the geometric analogy with a waffle. They are commonly used in the USA for the foundation of houses or any light weight structure on shrink-swell soils and cost about 100\$/m² (2010). This paper presents a simple design procedure and associated charts for calculating the depth of the beams required to limit the differential movement of the foundation due to bending to an acceptable amount.

Some of the other foundation solutions used for buildings on shrink-swell soils are thin post tension slab on grade, slab on grade and on piles, and elevated structural slab (Fig.1). The thin post tension slab on grade (say 0.1 m thick) is a very good solution for flat surfaces which are not carrying any structures such as tennis courts. The thin post tension slab on grade is not a good solution for the foundation of light and relatively rigid

structures because, while post tensioning increases the maximum bending moment that the slab can resist compared to the same reinforced concrete slab and provides a minor improvement in stiffness, it is generally too flexible and leads to differential movements of the foundation incompatible with what a rigid structure can tolerate. This can lead to cracking in the walls of the structure. Of course, thick post-tensioned slabs can work well and post tensioning a reinforced concrete stiffened slab on grade increases the maximum bending moment that the slab can resist. The benefit associated with the added cost of post-tensioning a reinforced concrete stiffened slab is not clear. The slab on grade and on piles is not a good solution either as it anchors the slab on grade while the soil may want to swell. In this case the soil pushes up on the slab and the piles hold it down at the connections between the pile and the slab. Under these conditions, the slab is likely to break if swelling is excessive. If the soil shrinks a gap can appear below the slab on grade which loses its support. Since such slabs are not designed to take the load in free span they can fail under these conditions as well. The elevated structural slab on piles is a very good solution but can be expensive (about 200\$/m² in 2010), and represents an unnecessary expense for light structures. It is the solution of choice for more expensive structures. In the case of the elevated structural slab on piles, the soil can move up and down without impacting the structure since a gap of sufficient magnitude (sometimes 0.3 m or more) exists under the beams and the slab. The load is taken up by the piles which must be designed for the tension generated by the swelling of the soil which is typically more severe than the shrinking design case.

Of course no matter how well designed and constructed the foundation is for light structures on shrink-swell soils, some poor practices by the owner can be very detrimental to the structure including trees too close to the structure and poor drainage. Proper owner maintenance is important and requires some education of the owner.

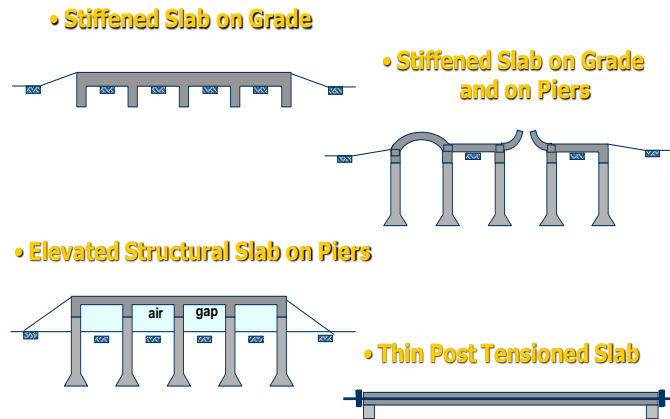


Figure 1. Some foundations used for light buildings on shrink-swell soils.

Development of the Design Approach

The primary design issues for stiffened slabs on grade are the sizing of the beams that stiffened the slab and the spacing of the beams. The beams are typically from 0.6 to 1.2 m deep, 0.15 to 0.3 m wide, and the spacing varies from 3 to 6 m. The slab itself is usually set at a thickness of 0.1 m. Any quality design for such a foundation must include the parameters related to the soil, the weather, the foundation, and the super-structure. The goal of such a design is to ensure that the stiffness of the foundation is such that the

movements due to swelling and shrinking of the soil under a given weather condition do not distort the super-structure excessively. The development of the design approach to size the beams and their spacing consisted of a number of research tasks which took place over the last 10 years. These tasks were.

1. Develop a simple way to obtain the coefficient of unsaturated diffusivity of the intact soil (lab) and the cracked soil (field).
2. Obtain a realistic shape of the mound that would be formed if the soil were to be partially covered by a perfectly flexible cover and were to shrink or swell in the free field
3. Simulate the effect of the weather on the soil in 5 cities over a 20 year period to obtain reasonable estimates of the maximum amplitude of variation of the suction over a 20 year period.
4. Place the foundation on top of that mound, solve the problem of soil-structure interaction and find out the maximum bending moment and deflection of the foundation slab. Perform an extensive parametric simulation study to find out what parameters are most important for the bending moment and the deflection.
5. Develop simple design charts based on the results of tasks 1 through 4 to obtain the beam depth and the beam spacing without having to use a computer.

Task 1 consisted of performing numerical simulations to develop the percent diffusion vs. time factor curves for the free shrink test much like the percent consolidation vs. time factor curves for the consolidation theory. These curves were used in conjunction with the free shrink test to obtain the coefficient of diffusivity of the intact soil. Then other numerical simulations were used to develop a correction factor for including the influence of cracks on the intact value of the diffusion coefficient.

Task 2 consisted of using an advanced form of Mitchell's theory (1979) to develop a more realistic solution for the equation describing the shape of the mound created when a flexible membrane covers partially a shrinking or swelling soil.

Task 3 required special numerical simulations using the FAO 56-PM method with weather input and soil input to obtain the maximum change in suction for several cities in the USA. These cities were selected because they have the most significant problems with shrink swell soils: San Antonio, Austin, Dallas, Houston, and Denver. College Station was added because it is the home of Texas A&M University. The weather input over the 20 year period considered included the rain fall, the air temperature, the wind speed, the relative humidity, and the solar radiation. An average vegetation cover was selected and the soil diffusion was varied over a reasonable range.

Task 4 consisted of running simulations with the foundation and its loading on top of the deformed mound as many have done before. The maximum bending moment in the stiffened slab and the deflections were obtain in a series of cases where many parameters were varied. This thorough sensitivity analysis gave a very clear indication of what parameters were most important and what parameters could be neglected within the precision sought.

Task 5 took advantage of all the results obtained to select the major factors and organize design charts which gave the beam depth for a given weather-soil index.

This paper covers Task 4 and Task 5 of the research effort and details the steps of the proposed design procedure with the charts. The results of the other tasks can be found in the work of Abdelmalak (2007) with further background found in Zhang (2004). Many design methods have been established for the design of stiffened slabs on shrink-swell soils; they include the Building Research Advisory Board method (BRAB 1968), the

Wire Reinforcement Institute method (WRI 1981), the Australian Standards method (AS 2870 1990, 1996), and the Post-Tensioning Institute method (PTI 1996, 2004). These design methods handle this problem by implementing different moisture diffusion, soil-weather interaction, and soil-structure interaction models. They all have advantages and drawbacks which lead the authors to develop this new method.

Numerical Simulation of the Soil-Slab Interaction

Finite element simulations for plates resting on a semi-infinite elastic continuum have been used to solve the problem of a slab resting on a soil mound since the 1970's. The starting point for all these simulations is to assume a certain soil mound shape. The mound shape equation developed in Task 2 was used to obtain the initial mound shape. Then, a 2D finite element simulation was carried out for a flat foundation slab centered on the mound. The output of this simulation was the deflected shape of the slab, the bending moment diagram across the slab and the shear force diagram across the slab.

Abdelmalak (2007) used the finite element package, ABAQUS/STANDARD, to simulate the problem. The mesh is shown in Figure 2 for the case where the soil is swelling around the edges of the slab (edge lift) as would happen in the winter time. Figure 3 shows the mesh in the case where the soil is shrinking around the edges of the slab (edge drop) as would happen in the summer time. A two dimensional plane strain condition was simulated and boundary conditions are shown in Figures 2 and 3. If L is the width of the slab, the mesh was $3L$ wide and $1.5 L$ deep and half the problem was simulated because of symmetry. The soil and the concrete were simulated as elastic materials and a load was imposed on the slab in addition to its weight.

As a simulation example, consider a plane strain problem for a foundation slab on an edge drop mound: The foundation slab has a width of $L=16$ m, an equivalent thickness of 0.38 m, a modulus $E_{\text{conc}} = 20000$ MPa, and it is loaded with 7.5 kPa. The foundation rests on an edge drop mound with a shape obtained from the equation derived in Task 2. The input parameters for the equation were a depth of active zone equal to 3.5 m, a free field imposed suction change of 1.82 pF at the boundary (or a suction change such that the ratio between the suction after and before is 66), and a soil with a field coefficient of diffusivity $\alpha_{\text{field}} = 0.02$ m²/day. The modulus of the soil for the finite element simulation was taken as $E_{\text{soil}} = 60$ MPa.

The initial and final soil mound profiles and the final slab profile for the example cited above are presented in Figure 4. Due to the slab weight and the load, the surface of the soil mound settles. Because the slab is stiff, a gap exists near the edge between the soil surface and the underside of the slab. The length of unsupported slab or gap length L_{gap} is about 3.5 m in this example. This over-hanging of the slab creates a significant bending moment and associated deflection. The bending moment and shear force diagrams across the slab are shown in Figure 5. As expected, the maximum bending moment coincides with the point of zero-shear. Note that the distance from the edge of the slab to the point of separation between soil and slab, L_{gap} , is smaller than the distance between the edge of the slab and the point of the maximum bending moment. In fact at the separation point the bending moment is only about half the maximum value. The reason is that the overhanging slab does not behave as a pure cantilever.

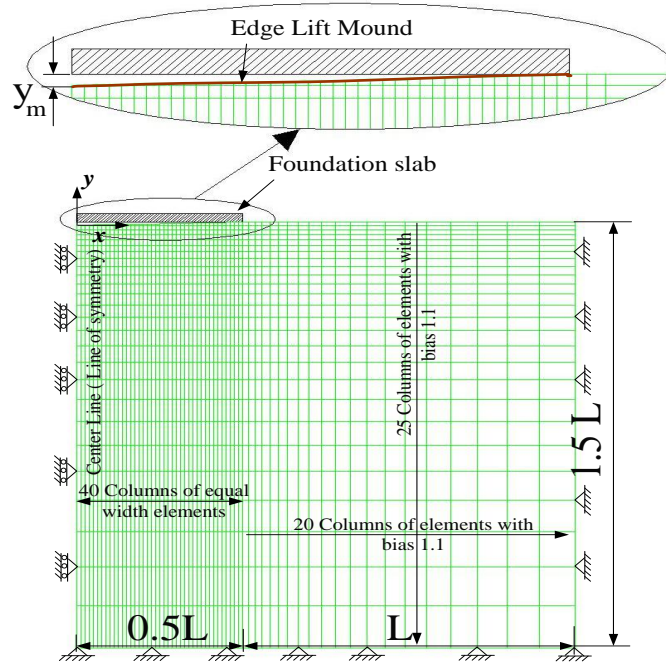


Figure 2. Geometry and boundary conditions for an edge lift case.

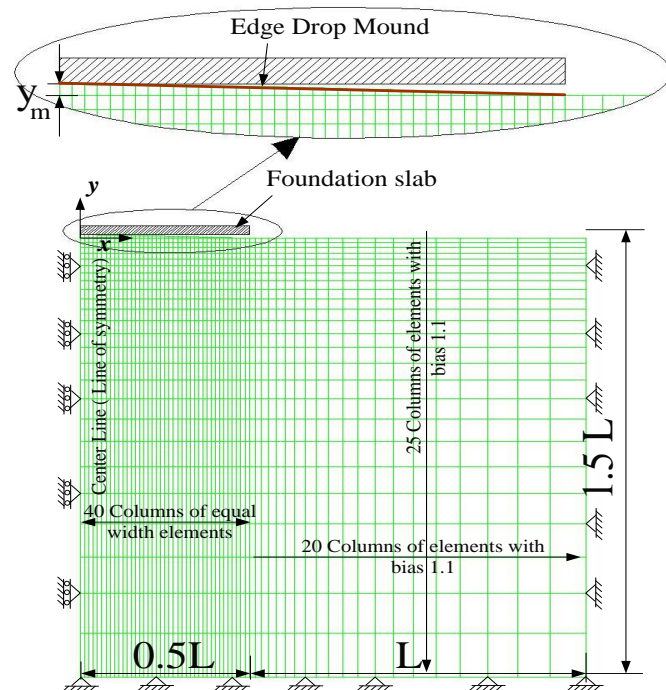


Figure 3. Geometry and boundary conditions for an edge drop case.

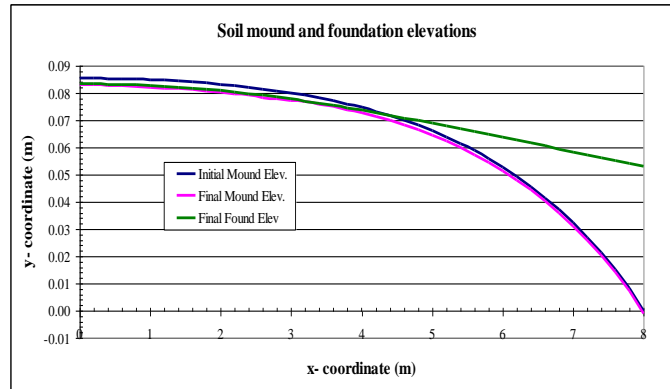


Figure 4. Initial and final soil mound profiles and final foundation slab profile.

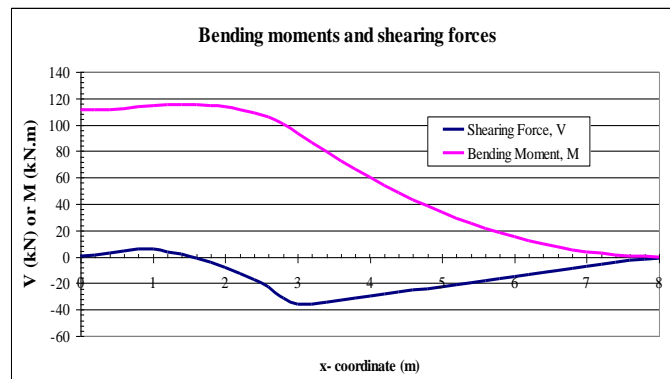


Figure 5. Bending moments and shearing forces results.

Influence Factors and Range of Values Simulated

Many factors are involved in the design of a slab on grade of shrink-swell soils. The weather factors include the change of soil suction at the ground surface in the free field, ΔU_0 , and the change of soil suction at the ground surface under the edge of the foundation, ΔU_{edge} . The soil factors include the soil modulus, E_{soil} , the shrink-swell index, I_{ss} (difference between the swell limit and the shrink limit), and the field coefficient of unsaturated diffusivity, α_{field} . The slab factors include the slab length, L , the slab bending stiffness EI , and the loading q . Obviously, in order to cover all the combinations of parameters, a very large number of simulation cases would have to be performed to develop a design procedure that addresses all these parameter effects. As a first step, a sensitivity study was undertaken to examine the influence of these parameters on the design of the foundation slab. This was done in hope to reduce the required number of simulations.

The range of the parameters included in the sensitivity study was chosen to realistically cover the anticipated variations. The change of soil suction at the ground surface in the free field, ΔU_0 , recommended by AS 2870 (1996) varies from 1.2 to 1.5 pF; this recommendation is based on databases of field measurements in Australia. To be safe the chosen range of ΔU_0 was expanded to be from 1 to 1.6 pF and five values were examined within that range 1, 1.15, 1.3, 1.45, 1.6 pF. The change of soil suction at the ground surface under the edge of the foundation, ΔU_{edge} was shown to be 0.5 times ΔU_0 (Abdelmalak 2007). Five depths of active moisture zones, H , were examined: 1.5, 2.5,

3.5, 4.5, and 5.5 m. The periodic time for the cyclic surface suction change due to weather variations was assumed to be 365 days.

Three soil moduli, E_{soil} were examined for the edge drop case (mounds resulting from soil shrinkage): 20, 60, and 100 MPa. These soil moduli are relatively high but were so chosen because drier soils tend to be stronger. For the edge lift cases (mounds resulting from soil swelling) the modulus values chosen for the sensitivity study were 6, 10, 15, 20 MPa. These moduli are smaller than the ones for the edge drop case because wet soils tend to be softer. The mound shape elevations for the edge lift case were scaled down by one half as will be explained later. Five soils were chosen with the following shrink-swell indices, I_{ss} : 75, 60, 45, 30, 15%, and the corresponding coefficients of saturated permeability were assumed to be $5 \text{ E-}10$, $7.5 \text{ E-}10$, $1 \text{ E-}09$, $2.5 \text{ E-}09$, and $5 \text{ E-}09$ m/sec respectively. This range of coefficients of saturated permeability was chosen to match the suggested values in Casagrande chart (Holtz & Kovacs 1981). The slope of the soil water characteristic curve (SWCC expressed as gravimetric water content versus suction), C_w was calculated using the shrink-swell index I_{ss} and the empirical relationship $C_w = 0.5 I_{ss}$ (Abdelmalak 2007). The field coefficient of unsaturated diffusivity, α_{field} , were chosen as 0.00724, 0.01244, 0.02042, 0.07110, and $0.26544 \text{ m}^2/\text{day}$.

The slab parameters were varied as follows: slab length, L , 4, 6, 8, 10, 12 m, beam depths 0.3, 0.6, 0.9, 1.2, and 1.5 m, beam width 0.3 m, and beam spacing 4 m. By equating the stiffness of these beam-stiffened slabs to the stiffness of a flat slab, a stiffness-based equivalent thickness can be calculated. The equivalent thicknesses of these beam stiffened flat slabs were, 0.127, 0.253, 0.3795, 0.506, and 0.633 m respectively. The load on the slab is given in terms of how much line load the beam has to sustain. This line load applied to the beam is obtained by multiplying the distributed pressure applied on the tributary area of the slab by the beam spacing (Fig. 6). The line loads imposed on the beams including dead weight were 2, 2.75, 3.5, 4.25, and 5 kN/m. The slab modulus of elasticity was 20000 MPa (concrete)

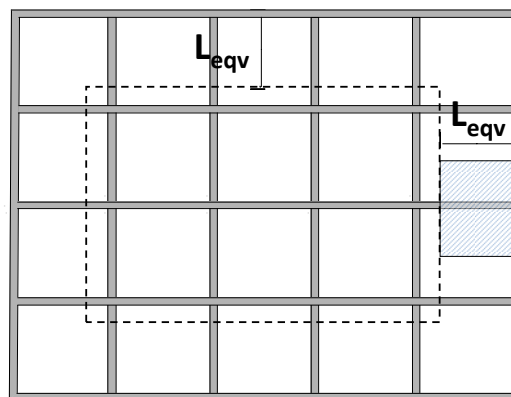


Figure 6. Tributary area used to calculate the line load on the beam.

Results of the sensitivity study

Before presenting the results, it is helpful to give the notation and definitions of all parameter (Fig. 7). Note that the parameters and their definitions are also listed in the nomenclature at the end of the paper.

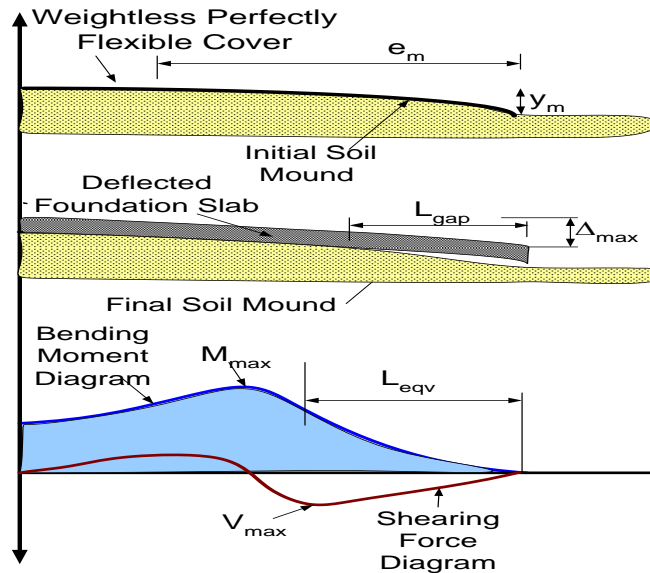


Figure 7. A sketch of a foundation slab on grade on a curved mound.

The reference case which was chosen corresponded to the median values of all the parameter (Table 1). The influence of each parameter variation will be compared to the reference case. The equivalent cantilever length, L_{eqv} , was chosen as the most important parameter in the design as it directly impacts the maximum bending moment and the maximum deflection. The influence of each parameter on L_{eqv} will be discussed next.

Table 1. Parameters for the reference case.

Parameter	$I_{ss}(\%)$	$H(m)$	$\Delta U_0(pF)$	$D(m)$	$L(m)$	$W_{imposed} (kPa)$
Reference case	45	3.5	1.3	0.9	8	3.5

Influence of the soil shrink-swell potential

Figure 8 shows the relationship between the soil shrink-swell potential, represented by the shrink-swell index, and the equivalent cantilever length. An increase in the shrink-swell index creates a non-linear monotonic increase in the equivalent cantilever length. The reason is that increasing the shrink-swell index increases the y_m values which in turn increases the soil mound distortion and consequently increases the foundation slab distortion. The average slope of the normalized equivalent cantilever length vs. the normalized shrink-swell index curve (Fig. 8) was 0.342 for the edge drop case and 0.369 for the edge lift case.

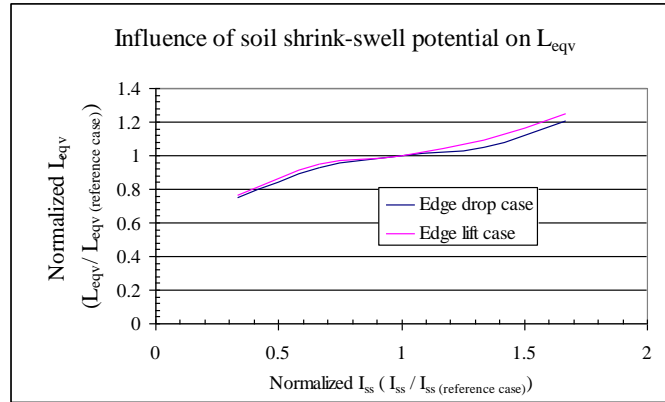


Figure 8. Influence of the soil shrink-swell potential on the equivalent cantilever length.

Influence of the depth of active moisture zone

Figure 9 shows the relationship between the depth of the active moisture zone and the equivalent cantilever length. An increase in the depth of the active moisture zone creates a non-linear monotonic increase in the equivalent cantilever length. The reason is that increasing the depth of the active moisture zone increases the y_m value which in turn increases the soil mound distortion and consequently the slab distortion. However, the slope of the normalized equivalent cantilever length vs. the normalized depth of the active moisture zone decreases as the depth of the active moisture zone increases.

The average slope of the normalized equivalent cantilever length vs. the normalized depth of the active moisture zone curve was 0.493 for edge drop case and 0.483 edge lift case. This indicates that the equivalent cantilever length seems to be somewhat more sensitive to the depth of the active moisture zone than to the soil shrink-swell potential; however, the depth of active moisture zone is also a function of soil shrink-swell potential

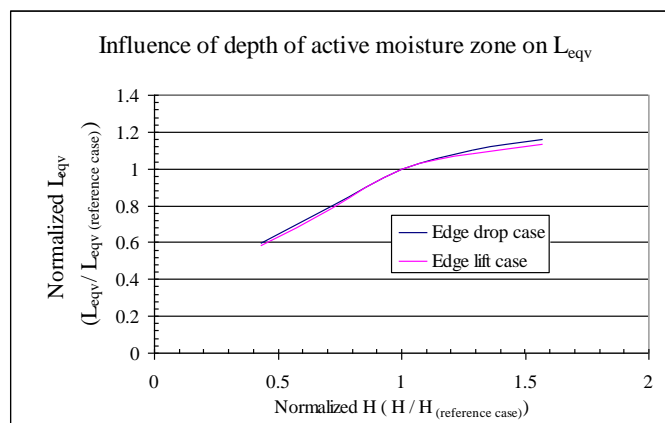


Figure 9. Influence of the depth of active moisture zone on the equivalent cantilever length.

Influence of the suction change at the ground surface

Figure 10 shows the relationship between the suction change at the ground surface vs. the resulting equivalent cantilever length. An increase in the soil surface suction change increases, almost linearly, the equivalent cantilever length. The average slope of the normalized equivalent cantilever length vs. the normalized soil surface suction change curve is 0.372 for edge drop case and 0.481 edge lift case. However, the range of the soil surface suction change was smaller than that of either the normalized shrink-swell index or the normalized of depth of active moisture zone.

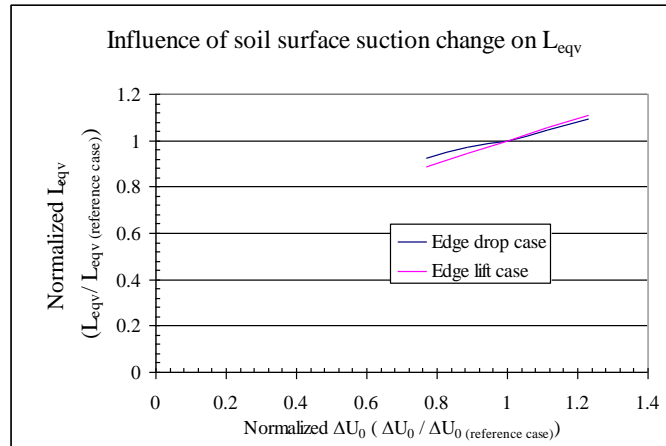


Figure 10. Influence of soil surface suction change on the equivalent cantilever length.

Influence of the slab stiffness

Figure 11 shows the relationship between the slab stiffness, represented by the depth of the stiffening beams, and the resulting equivalent cantilever length. An increase in beam depth significantly increases the equivalent cantilever length. The relationship is close to linear up to the average beam depth in this sensitivity study and then the curve becomes non linear. Note that the equivalent cantilever length cannot be larger than the half length of the slab which represents an upper bound for L_{eqv} . The average slope of the normalized equivalent cantilever length vs. the normalized beam depth curve was 0.628 for the edge drop case and 0.792 for the edge lift case. Considering the linear portion only, the slopes were 0.904 for edge drop case and 0.98 for the edge lift case.

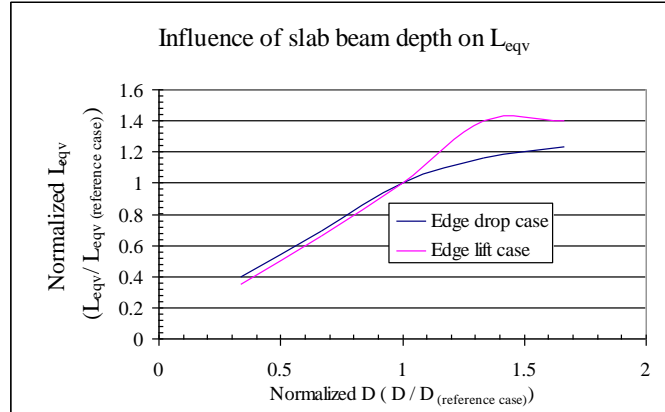


Figure 11. Influence of slab stiffness on the equivalent cantilever length.

Influence of the slab length

Figure 12 shows the relationship between the slab length and the resulting equivalent cantilever length. The equivalent cantilever length increases almost linearly with the slab length until it reaches a maximum value and then a constant value. The slab length affects two phenomena, moisture diffusion and slab curvature. For small 0.5 L/ H ratios, the difference in suction between the center of the slab and

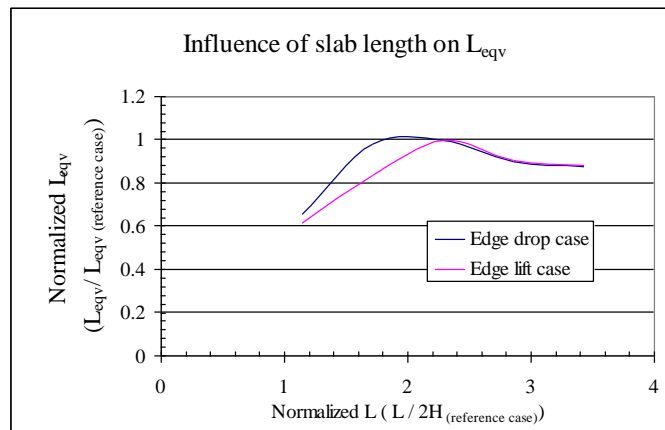


Figure 12. Influence of slab length on the equivalent cantilever length.

the edge of the slab is small and the curvature of the soil mound decreases. Consequently, the slab curvature decreases, and so does the equivalent cantilever length. On the other hand, increasing the slab length decreases the slab curvature and therefore the equivalent cantilever length. These two counteracting effects come to a balancing point at which the maximum equivalent cantilever length is reached. Hence, the influence of the slab length on the equivalent cantilever length can be addressed by introducing a reduction factor, F_{sl} , as shown on Figure 13 which can be viewed as an idealized form of Figure 12.

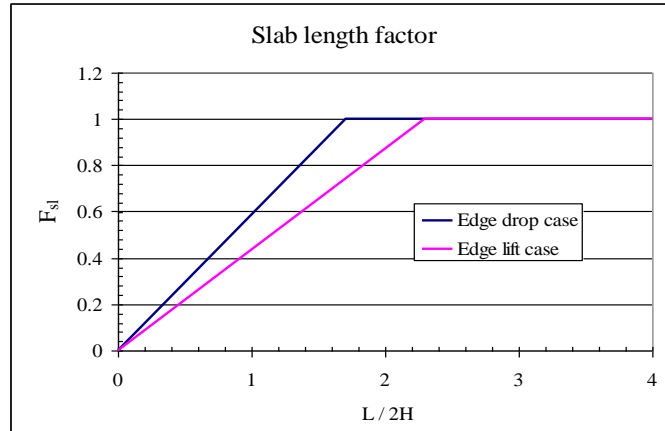


Figure 13. Slab length factor for reducing the equivalent cantilever length.

Influence of the slab load

Figure 14 shows the relationship between the slab load and the resulting equivalent cantilever length. The increase in slab load slightly decreases the equivalent cantilever length with a linear trend. Increasing the slab load compresses the soil mound which reduces its curvature thereby decreasing the resulting equivalent cantilever length. The average slopes of the normalized equivalent cantilever length and normalized slab beam depth curve were -0.141 for the edge drop case and -0.232 for the edge lift case.

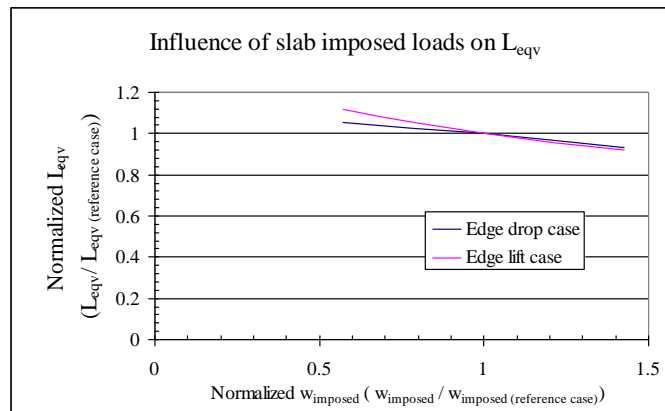


Figure 14. Influence of slab load on the equivalent cantilever length.

Influence of soil modulus of elasticity

For the edge drop case, the soil is shrinking and the increase in suction leads to a stiff soil. On the other hand in the edge lift case, the soil swells and the decrease in suction leads to a softer soil. As reasonable estimates, values of 20, 60, and 100 MPa were used for the soil modulus, E_s , of the stiff soil in the edge drop case and values of 5, 10, and 20 MPa for the softer soil of the edge lift case. Furthermore in the case of the edge lift case it was recognized that the pressure imparted on the soil by the slab and its load would lead to a mound shape exhibiting less curvature than the case of a free swelling soil. Figure 15 shows a typical influence of the vertical pressure on the percent swell of a soil. Note that, in Figure 15, the percent swell of the soil under very low

pressure is about 10% and the percent swell under 30 kPa of pressure is 5%. An arbitrary but seemingly reasonable reduction factor of 0.5 was applied on the free swell mound elevations before placing the slab and running the simulation of the edge lift case. Figure 16 shows the relationship between the soil modulus of elasticity and the resulting maximum bending moment. Figure 16 shows that the M_{max} increases when the soil becomes stiffer.

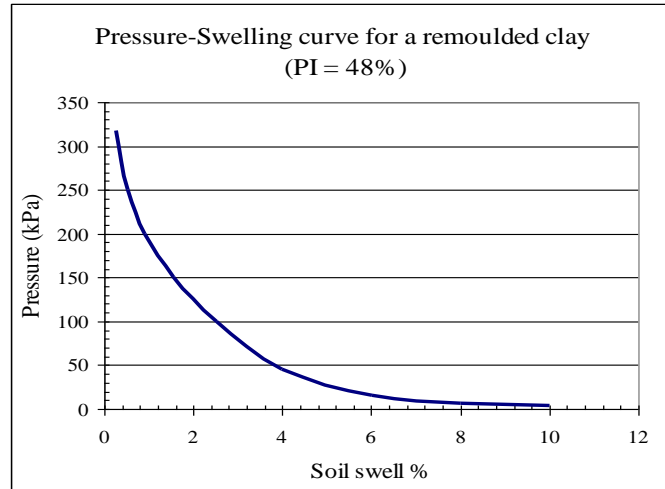


Figure 15. Typical pressure-swelling characteristic of clay (after Mitchell 1979).

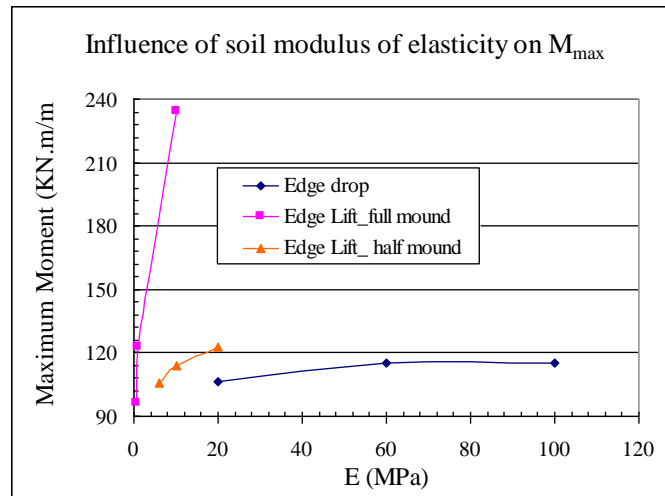


Figure 16. Influence of soil modulus of elasticity on M_{max} .

Conclusion of the sensitivity study

The sensitivity study showed that the following factors influence the design of slabs on grade on shrink-swell soils. These factors are cited in order of significance starting with the most significant factor: slab stiffness, depth of active moisture zone, shrink-swell potential, soil surface suction change, slab length, imposed loads, soil stiffness.

New Design Charts

Design parameters

The design parameters necessary to size the beams and their spacing are the maximum bending moment M_{\max} , the maximum shear force V_{\max} , and the maximum deflection Δ_{\max} of the slab. In the proposed design procedure, these quantities are presented by using the equations for a cantilever beam modified with a factor which makes them applicable to a slab on grade. These modification factors are based on all the numerical simulations. For a true cantilever beam, the equivalent cantilever length L_{eqv} would be the length of the cantilever beam, the maximum shear factor F_V would be one, and the maximum deflection factor $F_{\Delta_{\max}}$ would be 8. For the stiffened slab on grade, these factors were obtained from the numerical simulations.

$$L_{\text{eqv}} = (2M_{\max}/q)^{0.5} \quad (1)$$

$$F_V = \frac{V_{\max}}{qL_{\text{eqv}}} \quad (2)$$

$$F_{\Delta_{\max}} = \frac{qL_{\text{eqv}}^4}{\Delta_{\max} EI} \quad (3)$$

Note that L_{eqv} should be checked against $2H$ and if L_{eqv} is less than approximately $2H$ (Fig.13), L_{eqv} must be reduced according to Figure 13.

Soil-weather index

The sensitivity study showed that the main parameters to be included in the design procedure should be the shrink-swell index I_{SS} , the depth of the active zone H , the change of soil surface suction ΔU_0 , and the slab stiffness d_{eq} . The design parameters were the maximum bending moment (or equivalent cantilever length), the shear force, and the slab deflection. It was decided that the charts would have the design parameter on the vertical axis and a combined soil weather index on the horizontal axis. The chart would contain several curve each one referring to a given slab stiffness. So the next step was to develop a combined soil weather index $I_{\text{S-W}}$. Since the sensitivity study showed that the equivalent cantilever length increased with I_{SS} , H , and ΔU_0 , it was decided to define the soil-weather index as

$$I_{\text{S-W}} = I_{\text{SS}} \cdot H \cdot \Delta U_0 \quad (4)$$

Figure 17 shows the relationship between the soil-weather index and the equivalent cantilever length from the runs performed in the sensitivity study (median slab stiffness) (Abdelmalak 2007). A hyperbolic function, in the form of Equation 5 where L_0 , a , and b are constants, gave the best fit with a coefficient of determination equal to 0.944.

$$L_{\text{eqv}} = L_0 + \frac{aI_{\text{S-W}}}{1 + bI_{\text{S-W}}}, \quad R^2 = 0.944 \quad (5)$$

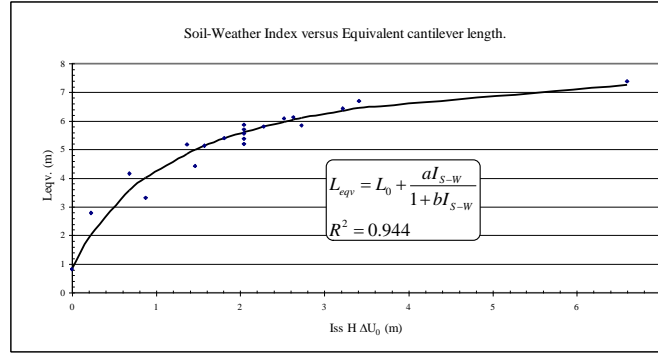


Figure 17. Relationship between the soil-weather index and the equivalent cantilever length.

Parametric analysis

Based on the success found in using the combined soil weather index (Fig. 17), a parametric analysis was undertaken to develop the design charts. Seven representative mounds were chosen including mounds with the minimum and maximum soil-weather indices to cover the whole possible range and five intermediate mounds. For each mound, five slab stiffnesses were chosen and numerically simulated for both the edge lift case and the edge drop case. Abdelmalak (2007) summarized the input parameters for the numerical simulations that were carried out to construct the design charts.

The slab stiffness was represented by the slab equivalent depth, d_{eq} . The slab equivalent depth d_{eq} represents the thickness of a flat slab which would have the same moment of inertia as the moment of inertia of a stiffened slab with a beam depth equal to D , a beam width equal to b and a beam spacing equal to S . The slab equivalent depth can be calculated by Equation 6:

$$S. d_{eq}^3 = b. D^3 \tag{6}$$

Suction based design charts

The large number of cases mentioned above were numerically simulated using ABAQUS/STANDARD (Abdelmalak 2007) and the output design parameters were plotted for the edge drop cases and for the edge lift cases, versus the soil-weather index. Note that in the design charts the soil weather index is used in terms of the suction change at the edge of the slab ΔU_{edge} rather than the suction change in the free field ΔU_0 . The numerical simulations indicated that ΔU_{edge} is equal to one half of ΔU_0 . For the edge drop case, Figure 18, Figure 19, Figure 20, and Figure 21 show the design charts for L_{eqv} , L_{gap} , $F_{\Delta max}$, and F_V respectively. For the edge lift case, Figure 22, Figure 23, and Figure 24 show the design charts for L_{eqv} , $F_{\Delta max}$, and F_V respectively.

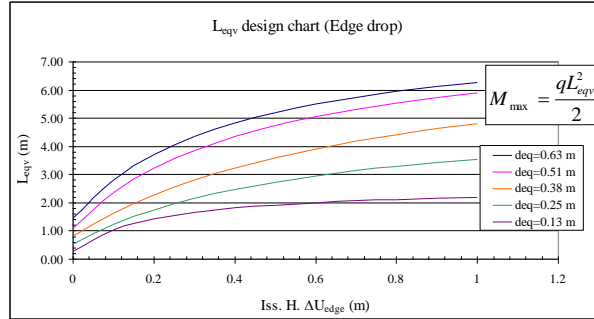


Figure 18. Equivalent cantilever length suction based design chart for edge drop case.

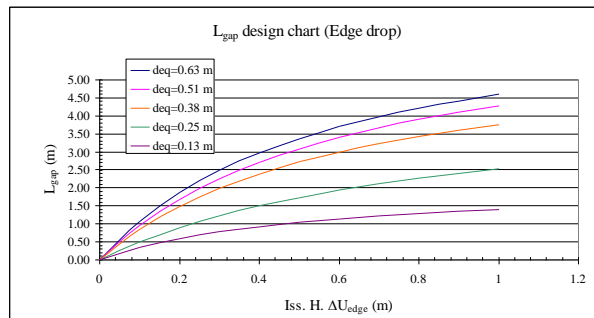


Figure 19. Unsupported length suction based design chart for edge drop case.

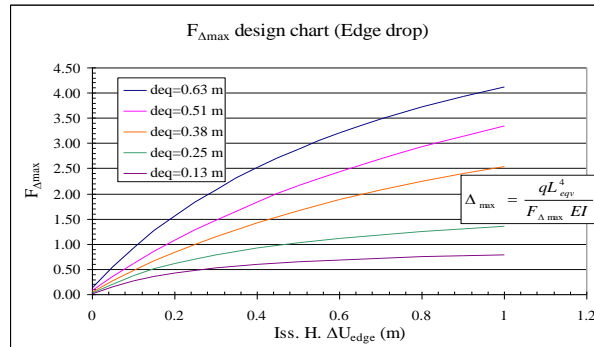


Figure 20. Maximum deflection factor suction based design chart for edge drop case.

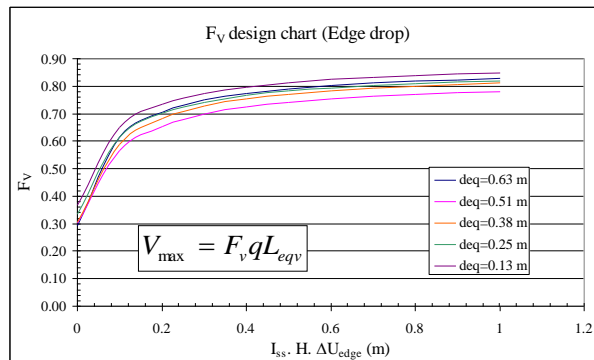


Figure 21. Maximum shear factor suction based design chart for edge drop case.

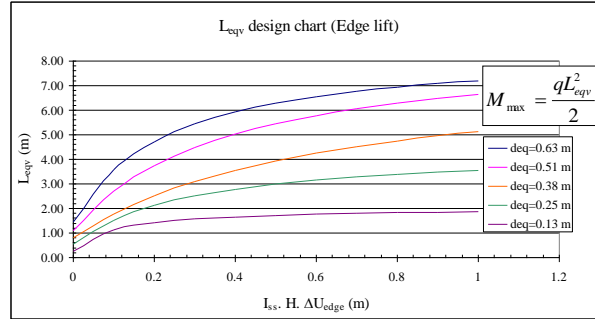


Figure 22. Equivalent cantilever length suction based design chart for edge lift case.

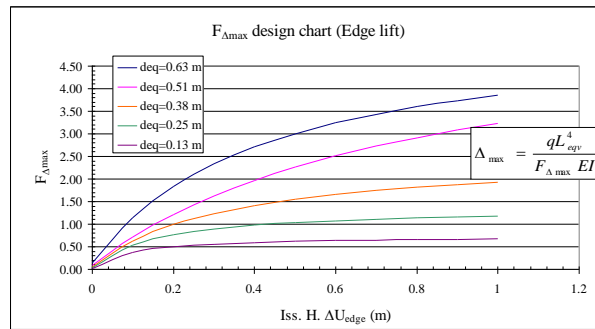


Figure 23. Maximum deflection factor suction based design chart for edge lift case.

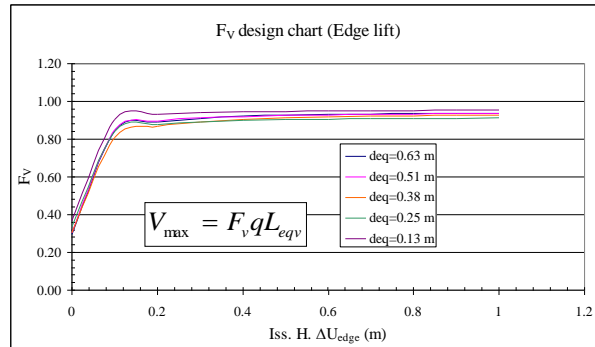


Figure 24. Maximum shear factor suction based design chart for edge lift case

Water content based design charts

The change in surface suction plays an important role in the mound shape equation; consequently it appears as an intrinsic component in the soil-weather index. However, measuring suction is more complicated than measuring water content, practitioners are more familiar with water content than with suction, and there is a much larger database of water content data than suction data. Therefore, it is convenient to have design charts in terms of water content in addition to having design chart in terms of suction. The soil water characteristic curve indicates that the change in suction ΔU_0 (pF) and the change in water content Δw_0 are linked by the specific water capacity C_w .

$$\Delta w_0 = C_w \cdot \Delta U_0 = 2 \cdot \Delta w_{edge} \tag{7}$$

Indeed the change in water content at the edge of the slab Δw_{edge} is one half of the change in water content in the free field Δw_0 since Equation 7 is linear and since $\Delta U_0 = 2 \cdot \Delta U_{edge}$ as mentioned before. Furthermore Abdelmalak (2007) showed that there is a simple empirical relationship between the specific water capacity C_w and the shrink-swell index I_{ss} :

$$C_w = I_{ss}/2 \tag{8}$$

Therefore,

$$I_{s-w} = 2 \cdot H \cdot \Delta w_0 = H \cdot \Delta w_{edge} \tag{9}$$

With Equation 9 it was easy to transform the suction based design charts into water content based design charts by simply replacing the definition of the soil weather index on the horizontal axis. An advantage of the water content base design charts is that consultants may have sufficient water content data in their files to estimate the depth of the active zone H and the change in water content Δw_0 . As an example Briaud et al. (2003) organized a water content database which gave average values of Δw_0 for three cities in Texas. Note that the design charts are given in terms of Δw_{edge} which is equal to one half of Δw_0 . For the edge drop case, Figure 25, Figure 26, Figure 27, and Figure 28 show the design charts for L_{eqv} , L_{gap} , $F_{\Delta max}$, and F_V respectively. For the edge lift case, Figure 29, Figure 30, and Figure 31 show the design charts for L_{eqv} , $F_{\Delta max}$, and F_V respectively.

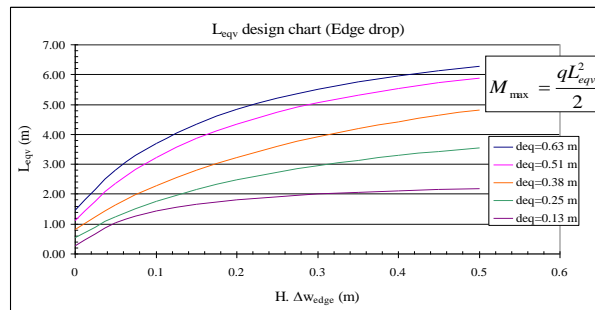


Figure 25. Equivalent cantilever length water content based design chart for edge drop case.

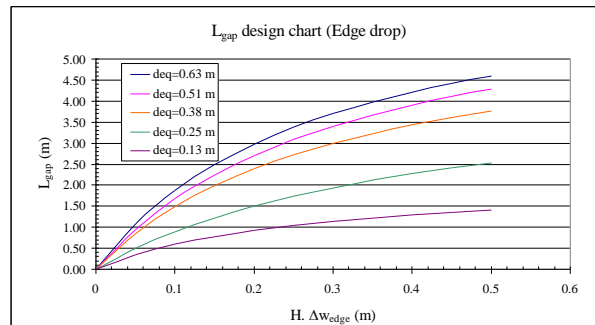


Figure 26. Unsupported length water content based design chart for edge drop case.

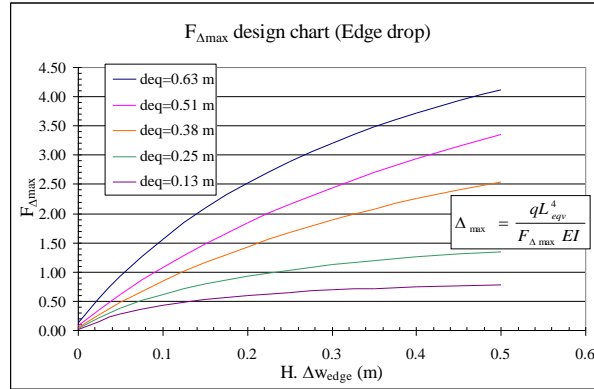


Figure 27. Maximum deflection factor water content based design chart for edge drop case.

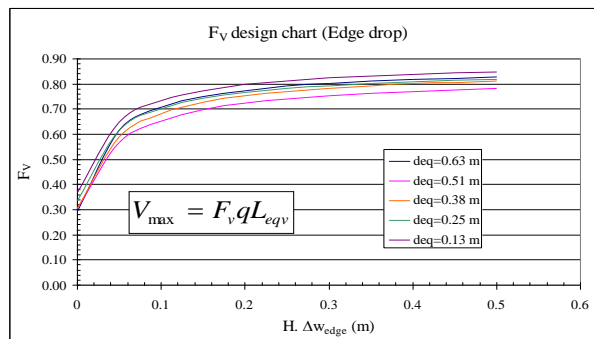


Figure 28. Maximum shear factor water content based design chart for edge drop case.

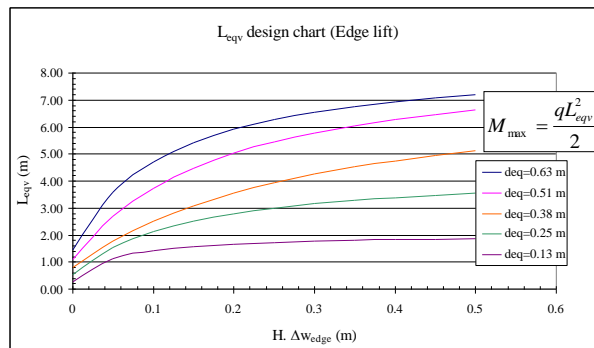


Figure 29. Equivalent cantilever length water content based design chart for edge lift case.

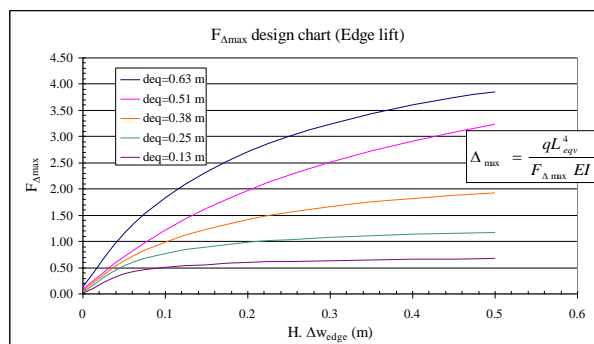


Figure 30. Maximum deflection factor water content based design chart for edge lift case.

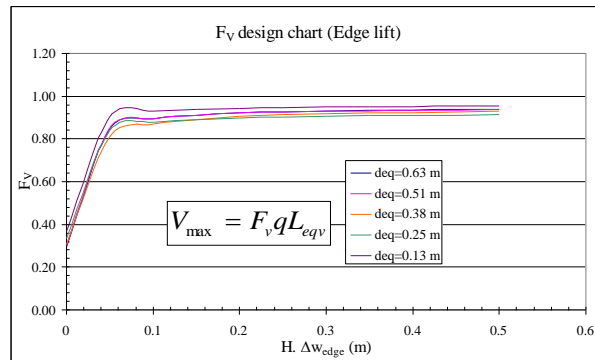


Figure 31. Maximum shear factor water content based design chart for edge lift case.

Design Example

Note that the design process advances by trial and error in the sense that the beam dimension and spacing are assumed and then the resulting deflection is calculated and checked against the distortion criterion. If the deflection criterion is not met, a larger beam depth is assumed. The input data for this example consists of the soil weather data and the slab data:

Soil and weather data:

- Depth of movement zone, $H = 3.0$ m
- Soil surface water content change $\Delta w_0 = 20\%$

Slab data:

- Slab dimensions = 20×20 m
- Beam spacing, $s = 3.0$ m (for both directions)
- Beam depth, $h = 1.2$ m
- Beam width, $b = 0.3$ m
- Slab load, $w = 10$ kPa

The calculations then proceed with the Soil-Weather Index I_{s-w} calculations

$$\Delta w_{edge} = 0.5 \Delta w_0 = 0.5 \times 0.2 = 0.1 \text{ or } 10\%$$

$$I_{s-w} = \Delta w_{edge} \times H = 0.1 \times 3 = 0.3 \text{ m}$$

and then the slab bending stiffness

$$EI = E b h^3 / 12 = 2 \times 10^7 \times 0.3 \times 1.2^3 / 12$$

$$= 8.64 \times 10^5 \text{ kN.m}^2$$

which leads to the equivalent slab thickness

$$b h^3 / 12 = s d_{eq}^3 / 12$$

$$d_{eq} = h (b/s)^{1/3} = 1.2 (0.3/3)^{1/3} = 0.56 \text{ m}$$

The values of the design parameters are read on the water content charts for the edge drop case

- $L_{eq} = 5.3$ m for maximum moment
- $L_{gap} = 3.6$ m for information
- $F_{\Delta max} = 2.9$ for maximum deflection
- $F_v = 0.8$ for maximum shear

The maximum bending moment is calculated as

$$\begin{aligned} q &= 10 \times 3 = 30 \text{ kN/m line load on the beam} \\ M_{\max} &= 0.5 q L_{\text{eq}}^2 = 0.5 \times 30 \times 5.3^2 \\ &= 421.3 \text{ kN.m} \end{aligned}$$

The maximum deflection is calculated as

$$\begin{aligned} \Delta_{\max} &= q L_{\text{eq}}^4 / F_{\Delta_{\max}} EI \\ &= 30 \times 5.34 / 2.9 \times 8.64 \times 10^5 \\ \Delta_{\max} &= 9.5 \times 10^{-3} \text{ m} \end{aligned}$$

The maximum shear force is calculated as

$$V_{\max} = F_v q L_{\text{eq}} = 0.8 \times 30 \times 5.3 = 127.2 \text{ kN}$$

This results in a distortion of

$$\begin{aligned} 0.5L / \Delta_{\max} &= 10 / 9.5 \times 10^{-3} = 1050 \\ L_{\text{eq}} / \Delta_{\max} &= 5.3 / 9.5 \times 10^{-3} = 558 \end{aligned}$$

Ratios less than 450 are typically acceptable according to the American Concrete Institute. This ratio however depends on the type of structure and the local code should be used for this step. Since L is much larger than 2H there is no need for a reduction of L_{eq} . This complete the design for the edge drop case. The edge lift case would proceed similarly. This example shows how simple the proposed method is. Note that this example is an extreme case as a Δw_0 of 20% corresponds to extreme weather conditions. This is why the beam depth is significant.

References

- Abdelmalak R. 2007. *Soil structure interaction for shrink-swell soils -A new design procedure for foundation slabs on shrink-swell soils*, Ph.D. dissertation, Department of Civil Engineering, Texas A&M University, College Station, TX.
- Australian Standard (AS2870). 1990. *Residential Slabs and Footings, Part 2: Guide to Design by Engineering Principles*, AS 2870.2 Standard House, Sydney NSW, Australia.
- Australian Standard (AS2870). 1996. *Residential Slabs and Footings*, AS 2870 Standard House, Sydney NSW, Australia.
- Briaud, J.-L., Zhang, X., and Moon, S. 2003. Shrink Test- Water Content Method for Shrink and Swell Predictions. *ASCE Journal of Geotechnical and Geoenvironmental Engineering*, 129(7): 590-600.
- Building Research Advisory Board (BRAB). 1968. *National Research Council Criteria for Selection and Design of Residential Slabs-on-Ground*, U.S. National Academy of Sciences Publication 1571.
- Holtz, R. D., and Kovacs, W. D. 1981. *An Introduction to Geotechnical Engineering*, Prentice-Hall, Englewood Cliffs, N.J., 180.
- Mitchell, P. W. 1979. The structural analysis of footings on expansive soils. *Research Report No. 1*, K. W. G. Smith and Assoc. Pty. Ltd., Newton, South Australia.
- Post-Tensioning Institute (PTI). 1996. *Design and Construction of Post-Tensioned Slabs-on-Ground*, 2nd Ed., Phoenix, AZ, USA,.
- Post-Tensioning Institute (PTI). 2004. *Design and Construction of Post-Tensioned Slabs-on-Ground*, 3rd Ed., Phoenix, AZ, USA.
- Wire Reinforcement Institute (WRI). 1981. *Design of Slab-on- Ground Foundations*, Findlay, Ohio, USA, August.
- Zhang, X. 2004. *Consolidation theories for saturated-unsaturated soils and numerical simulation of residential buildings on expansive soils*, Ph.D. dissertation, Department of Civil Engineering, Texas A&M University, College Station, TX.

Nomenclature

The following list gives the parameters associated with this paper and their definitions. Figure 7 illustrates their definition:

B	beam width
D	total beam depth
d_{eq}	thickness of a flat slab with the same moment of inertia as the stiffened slab
e_m	edge moisture distance. (Distance from the edge of the slab to the point where the water will penetrate horizontally below a weightless perfectly flexible cover)
EI	bending stiffness of the slab product of the modulus of elasticity of the slab material and the moment of inertia of the slab
$F_{\Delta_{max}}$	maximum deflection factor, $F_{\Delta_{max}} = \frac{qL_{eqv}^4}{\Delta_{max} EI}$ This factor is 8 for a cantilever beam but will be different for the slab on grade since it is not exactly a cantilever situation
F_V	maximum shear factor, $F_V = \frac{V_{max}}{qL_{eqv}}$. This number would be 1 for a cantilever beam but will be different for the slab on grade since it is not exactly a cantilever situation
H	depth of active zone. (Depth to which the variation of water content or suction will create movement of the soil)
I_{ss}	shrink-swell index. (Range of water content between the shrinkage limit obtained in a free shrink test and the swell limit obtained in a free swell test. The shrink=swell index is a very good indicator of a soil shrink-swell potential)
Q	total line load applied to the beam by the slab over the tributary area in Figure 6 (including dead weight of slab and imposed loads). $q = s.w$
L_{eq}	equivalent cantilever length. (Length of slab which gives the maximum bending moment in the beam when using the cantilever beam formula $M_{max} = qL_{eqv}^2/2$)
L_{gap}	unsupported length. (Length of slab without soil support underneath it)
M_{max}	maximum bending moment in the slab
S	beam center to center spacing
V_{max}	maximum shear force in the slab
W	average pressure generated by the slab weight and the load on the slab
y_m	vertical movement. (Difference in elevation due to swelling or shrinking between the two extremities of the e_m distance)
Δ_{max}	difference in elevation between the center of the slab and the edge of the slab
ΔU_{edge}	change in suction at the ground surface at the edge of the slab
ΔU_0	change in suction. (Change in suction in pF (log units) in the free field at the ground surface)
Δw_{edge}	change in water content at the ground surface at the edge of the slab
Δw_0	change in water content. (Change in water content in the free field at the ground surface)